Single source emission of proton projectile fragments in nucleus–emulsion interactions*

Zhang Dong-Hai(张东海)†, Li Jun-Sheng(李俊生), and Li Hui-Ling(李惠玲)

Institute of Modern Physics, Shanxi Normal University, Linfen 041004, *China*

(Received 29 March 2012; revised manuscript received 26 May 2012)

The projected angular distribution and transverse momentum distribution of proton projectile fragments produced in 3.7A GeV ^{16}O, 500A MeV ^{56}Fe, and 1.7A GeV ^{84}Kr induced by different kinds of emulsion target (H, CNO, and AgBr) interactions are investigated. It is found that the projected angular distribution and transverse momentum distribution can be well represented by a single Gaussian distribution. Comparison of transverse momentum distribution with the Maxwell–Boltzmann distribution reveals that proton projectile fragments are emitted from a single-temperature emission source. The temperature is different for different colliding systems, and linearly depends on the target size.

Keywords: nucleus–nucleus collision, proton projectile fragments, projectile fragmentation, nuclear emulsion

PACS: 05.30.Rt, 52.25.Tx, 52.20.Hv **DOI:** 10.1088/1674-1056/21/11/110501

1. Introduction

The particle production in relativistic nucleus–nucleus collisions have been extensively studied in recent years. Most of the studies have concentrated on particle production in the participant region with the goal of examining possible signals of quark gluon plasma (QGP). Studies on projectile fragmentation in spectator regions have received less attention. Based on the participant–spectator concept[1] and the simple fireball model,[2] the projectile and target sweep out cylindrical cuts through each other. Raha *et al.*[3] proposed that during the separation of spectators from participants, there must be some intercommunication between them, which results in the excitation of the spectators. Since this communication is strongly dependent on whether the participants form a QGP, the energy imparted in terms of temperature to the spectators may carry characteristic information with regard to the formation of a QGP in the participant region. They have proposed that observations of two quite different temperatures in the projectile-fragmentation region may be explained as a possible signal for the production of a QGP, and suggested the measurements of transverse momenta of proton projectile fragments (PFs) and helium PFs produced in high-energy nucleus–nucleus collisions as a method of searching for the occurrence of two temperatures.

The transverse momentum distribution of helium PFs has been studied by many experimental groups,[4−10] two distinctly different temperatures have been observed. These studies support the idea of Raha *et al.*[3] and seem to be an experimental signature of the QGP. For the transverse distribution of proton PFs produced in nucleus–nucleus collisions, a single-temperature emission source (cold source) is observed in 3.7A GeV ^{12}C[11] and 60A GeV ^{16}O[12] induced emulsion interactions, respectively. However, experiments performed by Nadi *et al.*[13] and Barrette *et al.*[14] produced two emission sources (cold and hot sources) instead of a single-temperature emission source (cold source). E802 collaboration[15] have studied the emission of proton PFs in Si–Au collisions at 14.6A GeV/c, a single-temperature emission source (hot source) is observed. Furthermore, two groups[16,17] have also studied the emission of proton PFs in electromagnetic dissociation of 200A GeV ^{16}O and ^{32}S in emulsion, and two temperature emission sources are observed in their data sets. Hence, more statistical experimental investigations are needed for the emission of proton PFs in nucleus–nucleus collisions at different energies.

In this paper, we present a systematic investigation on the projected angular distribution and

*Project supported by the National Natural Science Foundation of China (Grant No. 11075100) and Shanxi Scholarship Council of China (Grant No. 2011-058).

†Corresponding author. E-mail: zhangdh@dns.sxnu.edu.cn

© 2012 Chinese Physical Society and IOP Publishing Ltd

transverse momentum distribution of proton PFs produced in interactions of 3.7A GeV ^{16}O, 500A MeV ^{56}Fe, and 1.7A GeV ^{84}Kr and different kinds of emulsion targets (H, CNO, and AgBr). The transverse momentum distribution is compared with Maxwell–Boltzmann distribution, and a clear signature of a single-temperature emission source is observed.

2. Experimental details

Three stacks of nuclear emulsions are used in the present investigation. One stack of N4 nuclear emulsions fabricated by the Institute of Modern Physics (Shanxi Normal University, China), was exposed horizontally to HIMAC, NIRS, Japan. The exposure beam is 500A MeV ^{56}Fe, and the ion flux is 3000 cm^{-2}. The other two stacks exposed by 3.7A GeV ^{16}O and 1.7A GeV ^{84}Kr were provided by the EMU-01 collaboration. The BA2000 and XSJ-2 microscopes with a 100× oil immersion objective and 10× ocular lenses were used to scan the emulsion plates. The tracks were picked up at a distance of 5 mm away from the edge of the plates, and carefully followed until they either interacted with emulsion targets or escaped from the plates. Interactions, which occured within 30 μm on the top or bottom surface of the emulsion plates, were not considered for the final analysis. In each interaction, all of the secondaries were recorded, which includes shower particles, target recoiled protons (grey track particles), target evaporated fragments (black track particles), and projectile fragments. Details of track classification can be found in our recent papers.[18,19]

Proton PFs are emitted into the forward cone with respect to the beam direction. The emission angle is less than the projectile fragmentation angle which is about 3° for 3.7A GeV ^{16}O, 12° for 500A MeV ^{56}Fe, and 5° for 1.7A GeV ^{84}Kr, respectively.

3. Experimental results and discussion

We use 2041 ^{16}O, 1321 ^{56}Fe, and 558 ^{84}Kr–emulsion unbiased inelastic events in present investigation. According to the number of heavy ionized particles $N_{\rm h}$, the events are classified into three categories. Events with $N_{\rm h} \leq 1$ mainly refer to interactions with a H target (interactions with free and quasi-free nucleons) and peripheral interactions with other targets (interactions with only one bound nucleon in the CNO or AgBr nuclei). Events with $1 < N_{\rm h} < 8$ refer to the interactions with the CNO targets and some admixture of peripheral AgBr interactions. Events with $N_{\rm h} \geq 8$ are only interactions with AgBr targets.

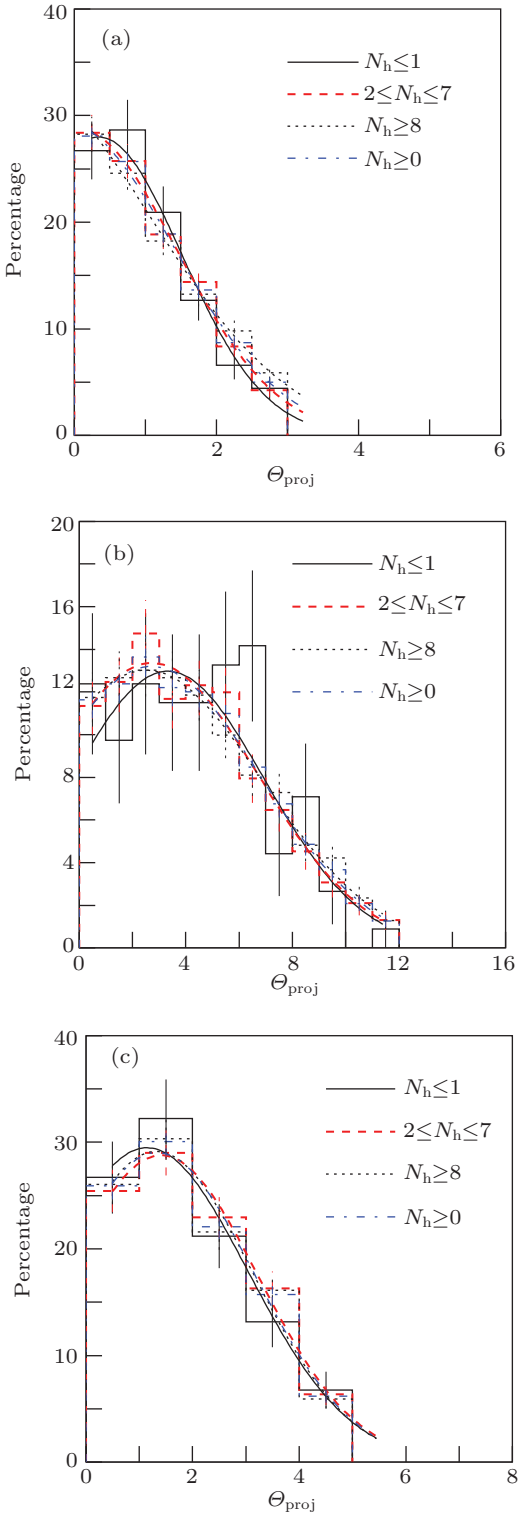


Fig. 1. Projected angular distribution of proton PFs for (a) 3.7A GeV ^{16}O, (b) 500A MeV ^{56}Fe, and (c) 1.7A GeV ^{84}Kr.

Figures 1(a)–1(c) show the projected angular distributions of proton PFs from 3.7A GeV ^{16}O, 500A MeV ^{56}Fe, and 1.7A GeV ^{84}Kr induced different kinds of emulsion targets (H, CNO, AgBr and emulsion) interactions, respectively. The experimental results can be well fitted by a single Gaussian distribution, which indicates that proton PFs come from a single emission source. The fitting parameters including χ^2/DOF are presented in Table 1, where the DOF means the degree of freedom of simulation.

Figures 2(a)–2(c) show the transverse momentum distributions of proton PFs from 3.7A GeV ^{16}O, 500A MeV ^{56}Fe, and 1.7A GeV ^{84}Kr induced different kinds of emulsion targets (H, CNO, AgBr, and emulsion) interactions, respectively. A single Gaussian distribution is fitted for all of the distributions, and the fitting parameters is presented in Table 1. We can see that the average transverse momentum of proton PFs increases with the increase of target size, and the width of the distribution also increases with the increase of the target size. According to the participant–spectator model, with the increase of the target size, the overlapped region and the contacted area increase, and the communication between participants and spectators increases as well. This results in the increase of the excitation energy of proton PFs, so the average transverse momentum of proton PFs increases.

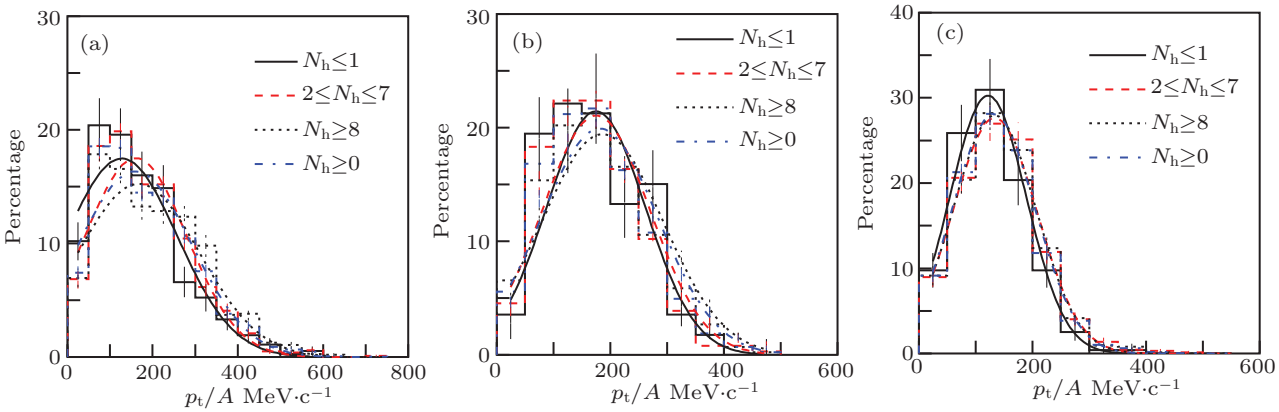


Fig. 2. Transverse momentum distribution of proton PFs from (a) 3.7A GeV ^{16}O, (b) 500A MeV ^{56}Fe, and (c) 1.7A GeV ^{84}Kr.

Table 1. Gaussian fitting parameters (average value and statistical error) of proton PFs projected angular and transverse momentum distributions.

Beam	Type of events	Projected angular distribution			Transverse momentum distribution		
		$\langle\theta_{\rm proj}\rangle$	$\sigma(\theta_{\rm proj})$	χ^2/DOF	$\langle p_{\rm t}\rangle$	$\sigma(p_{\rm t})$	χ^2/DOF
3.7A GeV ^{16}O	$N_{\rm h} \leq 1$	0.35 ± 0.29	1.17 ± 0.18	0.78	127.69 ± 12.40	130.88 ± 12.24	1.67
	$1 < N_{\rm h} < 8$	0.05 ± 0.29	1.40 ± 0.15	0.33	160.99 ± 4.98	119.93 ± 4.54	4.46
	$N_{\rm h} \geq 8$	-0.86 ± 1.11	1.94 ± 0.48	0.24	167.54 ± 6.79	141.65 ± 5.69	4.59
	$N_{\rm h} \geq 0$	-0.14 ± 0.26	1.53 ± 0.14	0.40	159.02 ± 4.01	133.21 ± 3.59	8.20
500A MeV ^{56}Fe	$N_{\rm h} \leq 1$	3.32 ± 0.83	3.64 ± 0.64	0.80	174.87 ± 8.53	86.97 ± 7.47	2.10
	$1 < N_{\rm h} < 8$	2.73 ± 0.43	4.00 ± 0.32	0.40	175.15 ± 3.69	94.53 ± 3.70	3.76
	$N_{\rm h} \geq 8$	2.52 ± 0.44	4.33 ± 0.31	0.22	186.33 ± 3.53	106.28 ± 2.98	1.08
	$N_{\rm h} \geq 0$	2.72 ± 0.28	4.11 ± 0.20	0.24	181.49 ± 2.48	102.46 ± 2.31	4.85
1.7A GeV ^{84}Kr	$N_{\rm h} \leq 1$	1.15 ± 0.38	1.90 ± 0.31	0.68	121.91 ± 4.90	67.53 ± 4.37	0.42
	$1 < N_{\rm h} < 8$	1.41 ± 0.18	1.82 ± 0.15	0.67	133.78 ± 3.29	73.80 ± 3.08	0.97
	$N_{\rm h} \geq 8$	1.32 ± 0.18	1.82 ± 0.14	1.87	133.32 ± 3.05	73.16 ± 2.71	0.91
	$N_{\rm h} \geq 0$	1.34 ± 0.12	1.83 ± 0.10	2.37	131.80 ± 2.04	72.91 ± 1.86	1.82

Based on the fireball model[2] of relativistic nucleus–nucleus collisions, the available energy in the center of mass heats the swept-out nucleons leading to a quasi-equilibrium fireball. This fireball can be described by a statistical (Maxwell–Boltzmann) distribution in the projectile rest frame. The transverse momentum of a projectile fragment is given by

$$p_{\rm t} = Am_0(\gamma^2-1)^{1/2}\sin\theta, \tag{1}$$

where A is the atomic number, m_0 the nucleon rest mass, γ the Lorentz factor of the projectile, and θ the emission angle of the projectile fragment with respect to the beam direction. If we assume that the emission of proton PFs is Maxwell–Boltzmann distribution in the projectile rest frame with a certain temperature T, then the integral frequency distribution of the square of the transverse momentum per nucleon is

$$\ln F(>p_{\rm t}^2) = -\frac{A}{2m_0T}p_{\rm t}^2. \tag{2}$$

The linearity of such a plot would be strong evidence for a single temperature.

Figures 3(a)–3(c) show the cumulative plots of $F(>p_{\rm t}^2)$ as a function of $p_{\rm t}^2$ for proton PFs from 3.7A GeV ^{16}O, 500A MeV ^{56}Fe, and 1.7A GeV ^{84}Kr induced different kinds of emulsion targets (H, CNO, AgBr and emulsion) interactions, respectively. All of the plots can be well fitted by a single Rayleigh distribution of the form

$$F(p_{\rm t}^2) = C\exp\left(-\frac{p_{\rm t}^2}{2\sigma^2}\right), \tag{3}$$

where $\sigma=\sqrt{2/\pi}\langle p_{\rm t}\rangle$, which is related to the temperature of the proton PFs emission source. The evidence of a single temperature is found in all of the data sets. The temperature and χ^2/DOF of simulation for different kinds of events are listed in Table 2. For comparison, the corresponding experimental results from 3.7A GeV ^{12}C[11] and 60A GeV ^{16}O–emulsion[12] interactions are also presented in the table. The experimental results show that the temperature of proton PFs emission source increases with the increase of the target size for a fixed projectile. For the same target, the temperatures of the proton PFs emission source decrease with increasing projectile mass at the three different beam energies. The general decreasing trend of the emission source temperature with increasing projectile mass is the same as that from Refs. [20] and [21] for the same beam energy. Song *et al.*[22] explained that the mass effect is caused by the Coulomb interaction because the system with larger projectile mass (and hence larger charge Z) has larger Coulomb pressure, which makes the system easy to separate. The dependence of the temperature of the proton PFs emission source on the target size is plotted in Fig. 4.

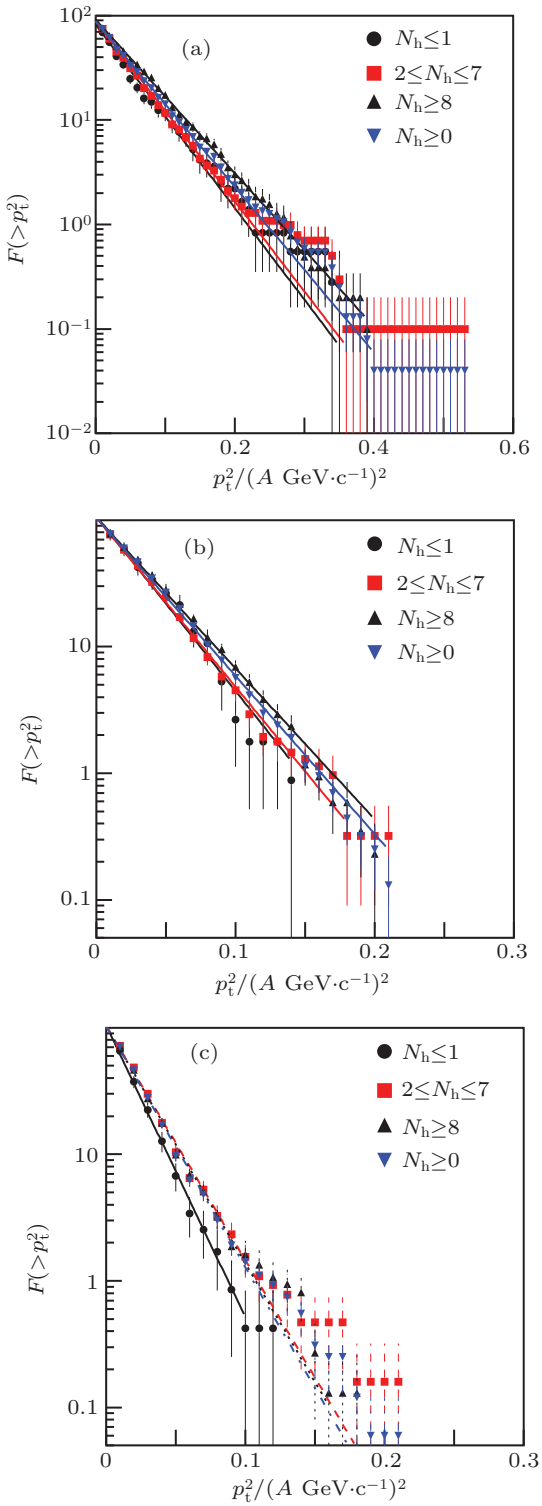


Fig. 3. (colour online) Cumulative plot of $F(>p_{\rm t}^2)$ as a function of $p_{\rm t}^2$ of proton PFs from (a) 3.7A GeV ^{16}O, (b) 500A MeV ^{56}Fe, and (c) 1.7A GeV ^{84}Kr.

The experimental results can be well fitted by a linear relation

$$T = a + bA_{\rm T}^{1/3}, \quad (4)$$

where $A_{\rm T}$ is the mass number of target. The fitting parameters are $a = 23.00 \pm 0.83$, $b = 1.75 \pm 0.23$, and $\chi^2/{\rm DOF} = 2.68$ for 3.7A GeV ^{16}O, $a = 15.38 \pm 0.68$, $b = 0.86 \pm 0.19$, and $\chi^2/{\rm DOF} = 0.27$ for 500A MeV ^{56}Fe, $a = 10.46 \pm 044$, $b = 0.47 \pm 0.13$, and $\chi^2/{\rm DOF} = 7.79$ for 1.7A GeV ^{84}Kr, respectively.

Table 2. Values of the single temperature from transverse momentum distributions of proton PFs.

Beam	Type of events	No. of events	Temperature/MeV	χ^2/DOF	Reference
3.7A GeV ^{16}O	$N_{\rm h} \leq 1$	326	26.3 ± 0.9	1.12	present work
	$1 < N_{\rm h} < 8$	788	26.7 ± 0.5	1.79	present work
	$N_{\rm h} \geq 8$	927	31.4 ± 0.4	0.53	present work
	$N_{\rm h} \geq 0$	2041	29.1 ± 0.3	2.20	present work
500A MeV ^{56}Fe	$N_{\rm h} \leq 1$	223	16.7 ± 0.8	0.59	present work
	$1 < N_{\rm h} < 8$	540	17.3 ± 0.4	0.59	present work
	$N_{\rm h} \geq 8$	558	19.4 ± 0.3	0.85	present work
	$N_{\rm h} \geq 0$	1321	18.5 ± 0.2	0.83	present work
1.7A GeV ^{84}Kr	$N_{\rm h} \leq 1$	93	10.0 ± 0.4	0.24	present work
	$1 < N_{\rm h} < 8$	233	12.5 ± 0.3	1.10	present work
	$N_{\rm h} \geq 8$	232	12.3 ± 0.3	1.17	present work
	$N_{\rm h} \geq 0$	558	12.1 ± 0.2	2.08	present work
3.7A GeV ^{12}C	$N_{\rm h} \geq 0$	400	8.0	0.10	[11]
60A GeV ^{16}O	$N_{\rm h} \geq 0$	475	58.0	0.10	[12]

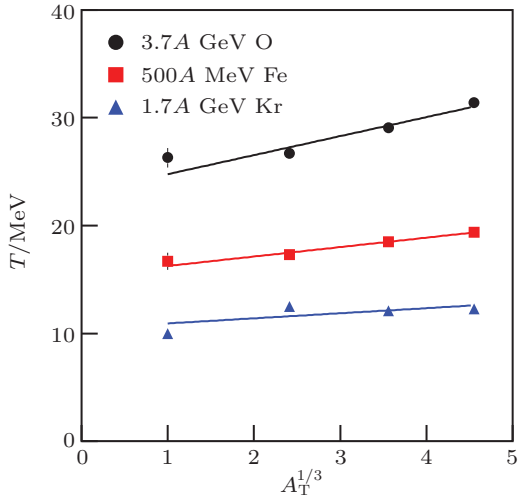


Fig. 4. (colour online) Dependence of the temperature of the proton PFs emission source on the size of the target.

According to the participant–spectator concept, it is assumed that when the interaction between projectile and target nuclei takes place, the projectile and target sweep out cylindrical cuts through each other. During the separation of the spectators from the participants, there is some intercommunication, which results in the excitation of the spectators. This excitation strongly depends on the contacted area of the colliding system. For a fixed projectile, the area of the contacted region increases with the increase of target size, so the excitation energy a projectile spectator receives is increased, which results in the temperature of the proton PFs emission source increasing. When the ratio of the projectile and target size increases, the relative influence of the received projectile spectator deceases. The experimental results indicate that a proton PFs emission source has a single temperature, which cannot be explained by Raha's suggestion. Thus, it seems that there is no QGP formed in the participant region in our investigated interactions.

According to the investigation by Su *et al.*,[21] the temperature of the emission source not only depends on the projectile and target mass, but also the isospin of the projectile. They found that the temperatures for the neutron-rich projectiles are larger than that for the neutron-poor projectiles. The isospin dependence of the isotope temperature in multi-fragmentation is weak, but can still be visible over a wide isotopic range. In the present paper, we cannot directly investigate the isospin effect of the emission source temperature because of the limited projectile, but we can investigate the dependence of the temperature of emission sources on the neutron-to-proton ratio N/Z by ignoring the difference between beam energies. Figure 5 shows the dependence of the temperature of the pro-

ton PFs emission source on the the neutron-to-proton ratio N/Z of a projectile; it is found that the temperatures decrease with increasing ratio N/Z for different target ranges, and this trend is the same as the result from Ref. [21] for stable projectile nuclides (Ca, Zr, Sn, and Pb at 600A MeV).

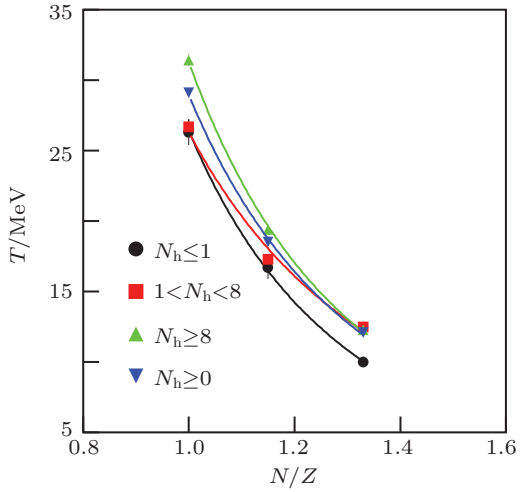


Fig. 5. (colour online) Dependence of the temperature of the proton PFs emission source on the neutron-to-proton ratio N/Z of the projectile.

4. Conclusion

From the studies on the emission of proton PFs in 3.7A GeV ^{16}O, 500A MeV ^{56}Fe, and 1.7A GeV ^{84}Kr induced using different kinds of emulsion target (H, CNO, AgBr, and emulsion) interactions, we can conclude that the projected angular distribution and transverse momentum distribution can be well fitted by a single Gaussian distribution, which indicates that the proton PFs are emitted from a single emission source. Comparison of the transverse momentum distribution with the Maxwell–Boltzmann distribution further reveals a single-temperature emission source of the proton PFs, which cannot be explained by Raha's idea. The temperature of the emission source increases with the target size and decreases with the projectile mass.

Acknowledgment

We are grateful to Prof. I. Otterlund at Lund University for supplying the emulsion plates, and to the staff of HIMAC, NIRS for exposing the emulsion stack.

References

[1] Bowman J D, Swiatecki W J and Tsang C F 1973 *Lawrence Berkeley Laboratory Report* LBL-2908
[2] Westfall G D, Gosset J, Johansen P J, Poskanzer A M, Meyer W G, Gutbrod H H, Sandoval A and Stock R 1976 *Phys. Rev. Lett.* **18** 1202
[3] Raha S, Weiner R M and Wheeler J W 1984 *Phys. Rev. Lett.* **53** 138
[4] Aggarwal M M, Bhalla K B, Das G and Jain P L 1983 *Phys. Rev.* C **27** 640
[5] Song F, Zhang D H and Li J S 2005 *Chin. Phys.* **14** 942
[6] Kamel S 1999 *Nuovo Cim.* A **112** 733
[7] Ghosh D, Roy J and Sengupta R 1988 *J. Phys.* G **14** 711
[8] Bhalla K B, Chaudhry M, Lokanathan S, Grover R K, Daftari I K, Kaul G L, Magotra L K, Prakash Y, Rao N K, Garpman S and Otterlund I 1981 *Nucl. Phys.* A **367** 446
[9] Baumgardt H G, Friedlander E M and Schopper E 1981 *J. Phys.* G **7** L175
[10] Joseph R R, Ojha I D, Tuli S K, Bhatia V S, Kaur M, Mittra I S, Sahota S S, Bhalla K B, Bharti A, Mookerjee S, Kitroo S and Rao N K 1989 *J. Phys.* G **15** 1805
[11] Ghosh D, Roy J and Ghosh K 1990 *Nuovo Cim.* A **103** 423
[12] Ghosh D, Das S K and Ghosh K 1997 *Nuovo Cim.* A **110** 565
[13] El-Nadi M, Abdelsaiam A, Hussien A, Shaat E A, Ali Moussa N, Abou Moussa Z, Kamel S, Abdel-Waged Kh, El Falaky E and Fayed M 1997 *Rad. Meas.* **28** 231
[14] Barrette J, Bellwied R, Braun-Munzinger P, *et al.* 1992 *Phys. Rev.* C **45** 819
[15] Abbott T, Akiba Y, Beavis D, *et al.* 1991 *Phys. Rev. Lett.* **66** 1567
[16] Singh G and Jain P L 1992 *Z. Phys.* A **334** 73
[17] Kamel S 1999 *Nuovo Cim.* A **112** 327
[18] Zhang D H, Cheng J X, Cheng B, Wang F, Wang Q, Zhang H Q, Xu R, Jia H M and Li X Q 2009 *Chin. Phys.* B **18** 531
[19] Li H L and Zhang D H 2009 *Chin. J. Phys.* **47** 27
[20] Sfienti C, Adrich P, Aumann T, *et al.* 2009 *Phys. Rev. Lett.* **102** 152701
[21] Su J and Zhang F S 2011 *Phys. Rev.* C **84** 037601
[22] Song H Q and Su R K 1991 *Phys. Rev.* C **44** 2505